ELSEVIER

Materials Science and Engineering A194 (1995) 179–186

MATERIALS SCIENCE & ENGINEERING A

The effect of niobium in solid solution on the transformation kinetics of bainite

G.I. Rees[a], J. Perdrix[b], T. Maurickx[b], H.K.D.H. Bhadeshia[a]

[a] *University of Cambridge Department of Materials Science & Metallurgy, Pembroke Street, Cambridge, CB2 3QZ, UK*

[b] *Sollac C.R.D.M., Rue du Comte Jean, Grande Synthe, Dunkerque, France*

Received 31 May 1994; in revised form 28 July 1994

Abstract

A study is made of the effect of niobium in solid solution in microalloyed austenite on the kinetics of transformation to bainite upon cooling, using a combination of dilatometry, scanning and transmission electron microscopy. The steels investigated are three laboratory melts with systematic variations in niobium concentration, and an industrial microalloyed grade. Results indicate that increasing niobium content retards the bainite transformation but that, while significant, this effect is rather small. A much more dramatic effect on bainite formation is produced by allowing a small amount of niobium carbo-nitride precipitation in the austenite before cooling.

Keywords: Niobium; Bainite

1. Introduction

Many authors [1–5] have reported the effect that additions of niobium have on the hardenability of steel. Most early studies concentrated on the effect of niobium on the onset temperature of allotriomorphic ferrite formation on cooling, and note that additions of niobium promoted bainitic structures at the expense of ferrite, by suppressing nucleation at austenite grain boundaries. The work of [5] indicates that by increasing the concentration of niobium in solution in austenite, the formation of allotriomorphic ferrite can be significantly retarded. However, a peak in the retardation effect is observed, with transformation kinetics accelerating for niobium concentrations beyond a critical value. In this case, the authors suggested that precipitation of niobium carbides during cooling preceded the ferrite transformation, and served as sites for its accelerated nucleation. In this respect the results are similar [3] to those observed for the retardation effect of boron on ferrite formation, where at high concentrations the retardation effect of boron disappears due to the preferential nucleation of ferrite on boride particles.

Recent work [6] revealed the effects of changing the extent of niobium carbide precipitation on the transformation kinetics of ferrite and *bainite* in a niobium-microalloyed steel. Initially the effects were interpreted as demonstrating the sensitivity of the formation of ferrite and bainite to the amount of niobium in solid solution in the austenite during cooling. In particular a strong correlation was demonstrated between the extent of carbide dissolution and the critical cooling rate required to avoid the formation of phases other than martensite (V_c). However, there is some ambiguity in the interpretation of these results, since, when considering only one steel, as the amount of niobium in solution is varied, there is a corresponding decrease in the fraction of carbide particles present in the austenite prior to transformation. It is possible, as austenitizing conditions are varied, that it is the changing number of these undissolved particles, acting as nucleation sites for transformation, that controls the hardenability.

In Thomas and Michal's work, the retardation of the allotriomorphic ferrite reaction when niobium was in solution was attributed to the so-called "solute-drag" effect, whereby the presumed segregation of niobium to the austenite–ferrite interface is assumed to modify

SSDI 0921-5093(94)09673-2

the diffusivity of the carbon as it is partitioned from the ferrite, decreasing the rate at which the interface can advance [7]. Indirect evidence of such segregation is provided by [3] who note that on repeated cycling of the austenitization and cooling treatments, the depression of the onset temperature of ferrite formation becomes more pronounced, despite no change in austenite grain size. This suggests increased inhomogeneity of niobium distribution with each cycle. The solute drag explanation is not satisfactory in the case of bainite, since such interface segregation of a substitutional element during transformation is considered incompatible with the reaction mechanism [8,9]. Other suggested retardation mechanisms, such as the stabilization of grain boundaries by segregation of misfitting niobium atoms, seem more plausible [10]. There is therefore a need to clarify previous results obtained in order to achieve a better understanding of the factors affecting transformations in steels containing niobium.

2. Experimental details

Two series of experiments were performed, using steels of composition listed in Table 1. The first series, to investigate the effect of varying the amount of niobium in solid solution in austenite on the transformation to bainite, used steels 1–3, which were laboratory melts, prepared to differ significantly only in niobium content. These steels were produced by vacuum induction melting, and were hot rolled to plate (dimensions 12 mm × 80 mm), with the finish rolling temperature being 900 °C. Following rolling the steel was reheated to 910 °C and air cooled.

The second series of experiments was to investigate the effect of carbide precipitation from the austenite phase on bainite transformation kinetics. These experiments used the commercial steel grade S355N, produced by Usinor-Sacillor, which we have labelled steel 4. The chemical composition of this grade is essentially similar to that of the laboratory melts, but with a higher niobium content. The rolling schedule used in the production of all four steels was identical.

For the first series of experiments, two austenitization treatments were used, at a temperature at which any niobium carbide in the microstructure should have dissolved. The thermal cycles are shown schematically in Fig. 1. CCT curves for 5% transformation were then determined by cooling to room temperatures at various rates. The different austenitization conditions were in order to produce two different grain sizes in each steel. Since the carbide dissolution temperature for the lowest niobium steel is expected to be lower than for the higher niobium steels, the grain size achieved by the austenitization treatment should be smaller as the niobium concentration is increased. On the other hand, the expected effect of niobium in solid solution is to retard transformation to ferrite and bainite. If the transformation kinetics of the highest niobium steel are visibly slower than for the lower-niobium steels then this will have to manifest itself over and above any effect due to the difference in grain size. In such a case, the retardation of transformation will be identified unambiguously as being due to niobium in solid solution. Previous work has also indicated [6] that for large austenite grains, the sensitivity of V_c to grain size is in any case rather low.

The second series of experiments used thermal cycles of the type illustrated in Fig. 2. Following austenitization at 1250 °C the specimens of steel 4 were held at various temperatures for a second-stage austenitization. For each second-stage temperature, two hold times were employed, arbitrarily chosen as 54 s and 460 s, before cooling to room temperature at various rates. The initial austenitization temperature was sufficiently high to cause dissolution of any niobium carbide present in the initial microstructure, so that any such particles present in the final microstructure should be due to precipitation during the second-stage holding. The critical cooling rate V_c was then determined as a function both of the second-stage austenitization temperature and of time.

The transformation was monitored using a Gleeble 1500 thermo-mechanical simulator, with cylindrical specimens of dimension 5 mm × 90 mm. The thermal cycle employed also cooled the specimens rapidly from

Table 1
The composition (wt.%) of the experimental steels used for dilatometry

Alloy	C	Si	Mn	NI	Mo	Cr	Cu	V	Ti	Nb	P	S
Steel 1	0.143	0.438	1.599	0.025	0.017	0.027	0.017	0.003	0.002	<0.001	0.022	0.003
Steel 2	0.142	0.437	1.577	0.024	0.016	0.026	0.017	0.003	0.002	0.011	0.022	0.003
Steel 3	0.149	0.445	1.607	0.026	0.016	0.027	0.018	0.003	0.002	0.026	0.024	0.003
Steel 4	0.152	0.467	1.545	0.025	0.00	0.02	0.014	0.003	0.003	0.035	0.021	0.004

the austenitization temperature (1250 °C) to 800 °C in order to minimize the time spent at higher temperatures. CCT curves are therefore shown with zero time corresponding to when the specimen reached 800 °C on cooling.

Metallographic samples were ground and polished by standard techniques. Scanning electron microscopy was performed on specimens etched by 2% Nital. Grain size determination was done by first revealing the prior austenite grain boundaries by etching with Bechet–Baujard reagent (aqueous picric acid + wetting agent) at 60 °C, then on a series of photomicrographs, the mean number of grains per unit area n_A was evaluated and related to the mean grain diameter d by the relation [11]

$$d = (n_A)^{-1/2} \text{ m}$$

The extent of carbide precipitation resulting from the two-stage austenitization treatments was investigated by taking carbon extraction replicas of the most rapidly cooled steel 4 specimens, following each austenitization treatment. These were examined under the transmission electron microscope.

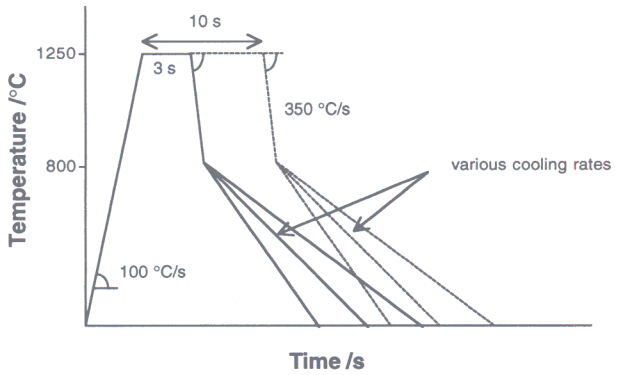

Fig. 1. Schematic representation of the thermal cycles applied to determine the CCT curves of steels 1–3.

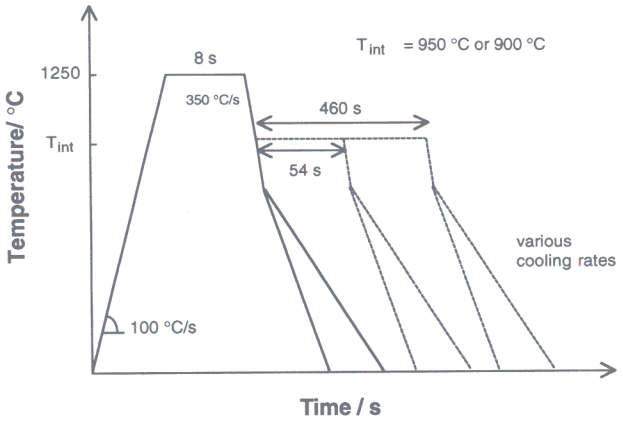

Fig. 2. Thermal cycles applies to steel 4 to investigate the effect of carbide precipitation on transformation of austenite.

3. Preliminary calculations

Preliminary calculations were performed in order to estimate the equilibrium Ae_3 temperature and the equilibrium dissolution temperature for niobium carbide for each steel. These calculations were done using the Thermocalc [12] phase diagram modelling package, and the solubility product relationship of [13] respectively. The solubility product expression used takes account of the effect of manganese on the carbide stability, i.e.

$$\log_{10}\{[\text{Nb}][\text{C}]\} - 0.248[\text{Mn}] = 1.8 - \frac{6770}{T}$$

where [Nb], [C] and [Mn] are the concentrations of niobium, carbon and manganese respectively (in weight %), and temperature T is in kelvin. The results are shown in Table 2.

4. Results and discussion

Table 3 gives the measured grain sizes of steels 1–3 following each austenitization treatment. The experimentally determined CCT curves for these steels following the 10 s and 3 s austenitization are shown in Figs. 3–8. These figures show smooth curves drawn through the time–temperature measurements corresponding to 5%, 25%, 50% and 75% transformation.

Table 2
Calculated phase boundary temperatures for the experimental alloys

Alloy	Phase boundary temperature (°C)	
	$(\alpha + \gamma + \text{NbC})/(\gamma + \text{NbC})$	$(\gamma + \text{NbC})/\gamma$
Steel 1	822	847
Steel 2	823	1081
Steel 3	822	1195
Steel 4	824	1245

Table 3
Austenite grain sizes (with standard errors) following the two austenitization treatments

Alloy	Mean grain diameter (μm)	
	$t_\gamma = 3$ s	$t_\gamma = 10$ s
Steel 1	184 ± 15	391 ± 35
Steel 2	110 ± 6	143 ± 10
Steel 3	116 ± 7	155 ± 15

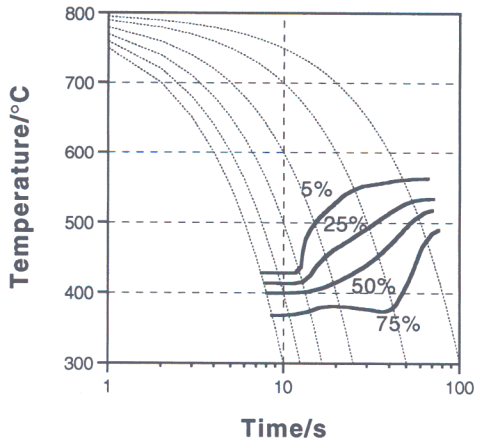

Fig. 3. Full CCT diagram for steel 1 following austenitization for 10 s at 1250 °C.

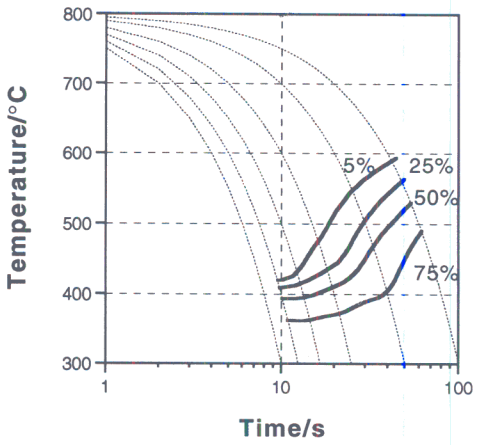

Fig. 6. Full CCT diagram for steel 2, following austenitization for 3 s at 1250 °C.

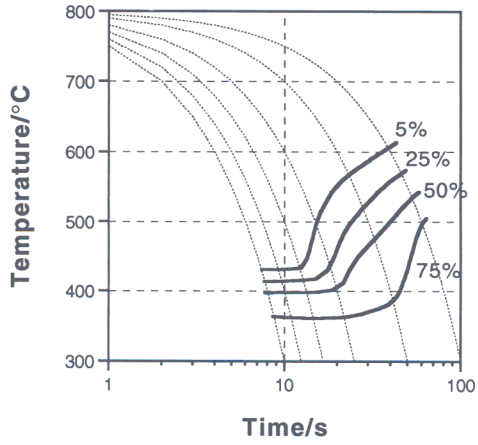

Fig. 4. Full CCT diagram for steel 1, following austenitization for 3 s at 1250 °C.

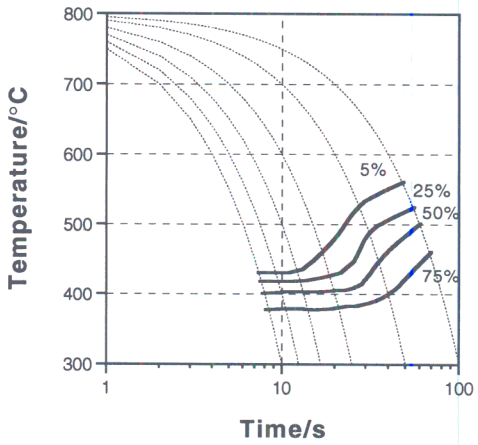

Fig. 7. Full CCT diagram for steel 3, following austenitization for 10 s at 1250 °C.

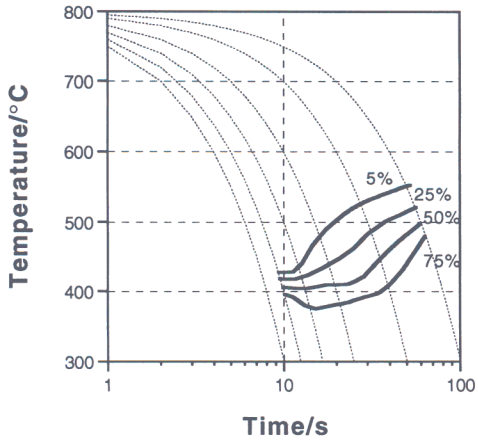

Fig. 5. Full CCT diagram for steel 2, following austenitization for 10 s at 1250 °C.

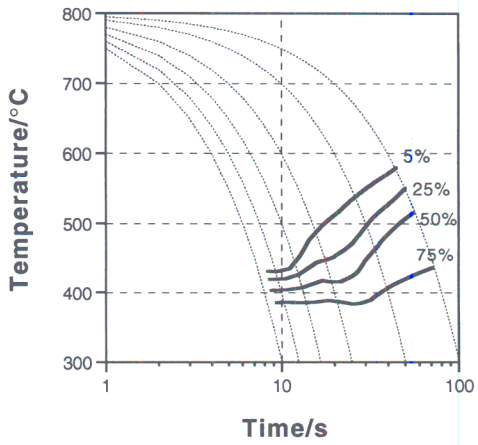

Fig. 8. Full CCT diagram for steel 3, following austenitization for 3 s at 1250 °C.

The method used to analyse the dilatometric data is given elsewhere [6].

To compare the effect of the different niobium concentrations in solution, Figs. 9 and 10 compare the 5% transformation curves for the three steels following austenitization at 1250 °C for 3 s and 10 s respectively. Examples of the microstructural effect of increasing the niobium content on transformation are shown in Figs. 11–14, which compare the microstructures of steel 1 and steel 3 cooled at 30 °C s^{-1} (Figs. 11 and 12 respectively) and 5 °C s^{-1} (Figs. 13 and 14 respectively).

Fig. 15 shows the CCT diagrams for steel 4 illustrating the effect of the second-stage austenitization temperature with the holding time of 460 s at 950 °C and 900 °C. For shorter holding times at these temperatures (54 s) the curves are not very different from that produced by direct cooling from 800 °C: i.e. identical thermal cycles but with no second stage holding. Increasing the holding time to 460 s has a dramatic accelerating effect on transformation.

4.1. *The effect of grain size and composition on transformation*

Within the experimental error, the grain sizes of steels 2 and 3 are essentially the same for both cycles, but differ markedly from those of steel 1. Since in all cases we are clearly above the grain coarsening temperature, precipitates such as niobium carbide therefore having dissolved, these differences may be attributable to the retarding interaction of niobium in solid solution with the growing austenite grains [14–16]. It is surprising though that steel 2 shows a slightly smaller grain size to steel 3.

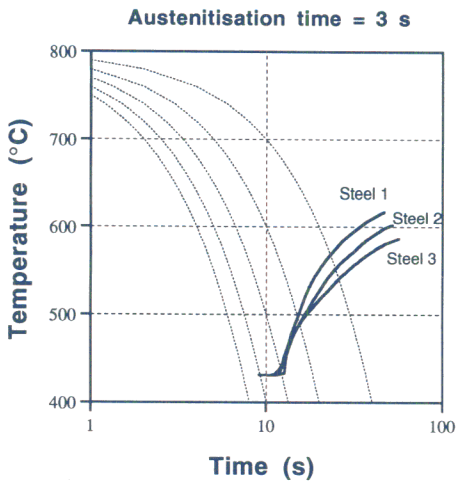

Fig. 9. CCT diagram for steels 1–3, following austenitization for 3 s at 1250 °C.

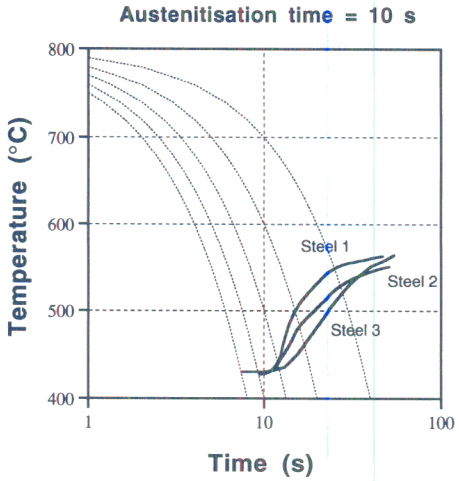

Fig. 10. CCT diagram for steels 1–3, following austenitization for 10 s at 1250 °C.

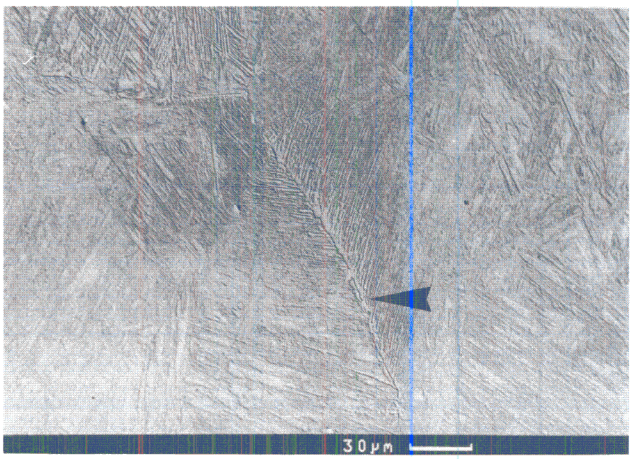

Fig. 11. Microstructure of steel 1 ([Nb] < 0.001 wt.%) cooled at 30 °C s^{-1} following austenitization at 1250 °C for 3 s.

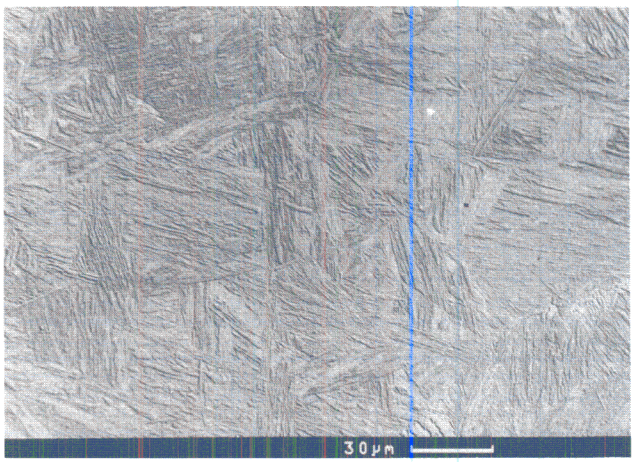

Fig. 12. Microstructure of steel 3 ([Nb] = 0.026 wt.%) cooled at 30 °C s^{-1} following austenitization at 1250 °C for 3 s.

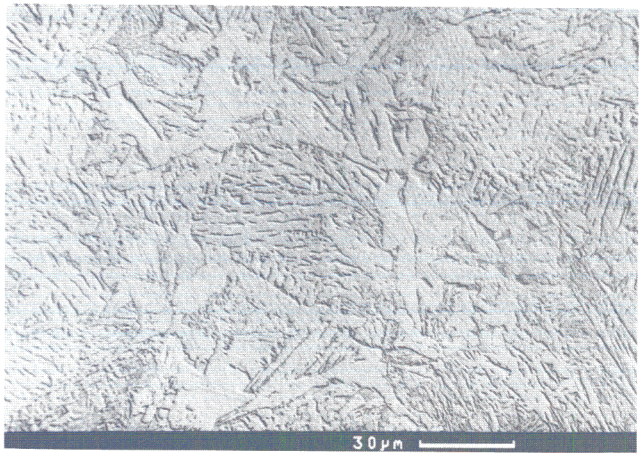

Fig. 13. Microstructure of steel 1 ([Nb] < 0.001 wt.%) cooled at 5 °C s^{-1} following austenitization at 1250 °C for 3 s.

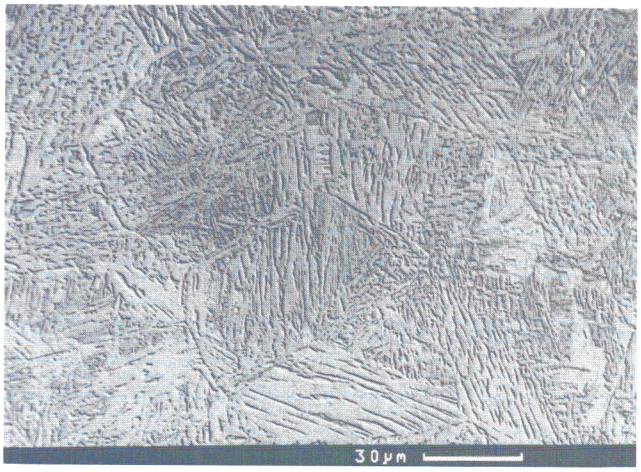

Fig. 14. Microstructure of steel 3 ([Nb] = 0.026 wt.%) cooled at 5 °C s^{-1} following austenitization at 1250 °C for 3 s.

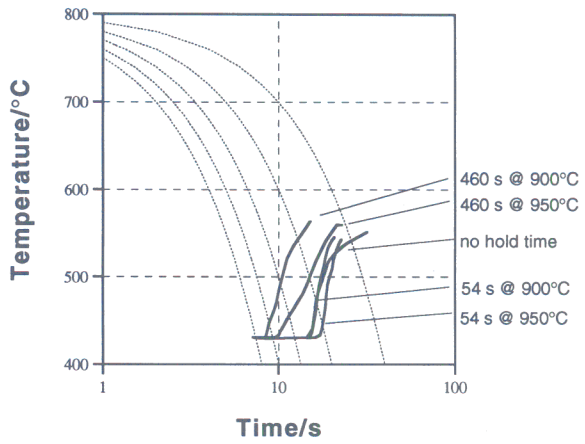

Fig. 15. CCT curves showing the effect on transformation kinetics of holding steel 4 at for 54 s and 460 s at 900 °C and 950 °C compared with specimens cooled directly from 800 °C.

From the CCT curves for steels 1–3 (Figs. 3–10) it can be seen that at the slower cooling rates, the larger-grained samples of each steel clearly begin to transform at lower temperatures, indicating a slower nucleation rate relative to the smaller-grained samples. As the critical cooling rate V_c is approached, however, the differences due to grain size become too small to measure accurately.

As a function of the concentration of niobium in solid solution, there is little difference in the determined values of V_c for all three steels. For the samples austenitized for 10 s at 1250 °C, a small tendency for increasing niobium content to retard transformation can be seen, even as V_c is approached (Fig. 10). In stark contrast however, the effect of holding steel 4 within the austenite/niobium carbide two-phase field is dramatic, and has a significant effect on the critical cooling rate. Indeed, the transformation kinetics of steel 4 after a second-stage holding time of 460 s at 950 °C or 900 °C are faster than those of the steel 1 (very low niobium content). The precipitation of carbides therefore seems to accelerate transformation over and above the effect expected if the mechanism of acceleration was simply the removal of niobium from solid solution in the austenite.

Despite the fact that V_c does not seem strongly affected by niobium in solution in the austenite, there is a small effect on microstructure. Comparing samples of steels 1 and 3 cooled at 30 °C s^{-1}, in steel 1 regions of grain boundary that have begun to nucleate bainite are far more common than in steel 3. An example of such a nucleating region from steel 1 is shown (arrowed) in Fig. 11. In comparison, the austenite grain boundaries in steel 3 are largely free of any signs of nucleation (Fig. 12). It is emphasized though that in both these samples the fraction of bainite that has formed is less than 5%, and that regions of nucleation are very rare. This effect is too small to be detected dilatometrically. A similar trend can also be seen with regards to allotriomorphic ferrite formation by comparing Figs. 13 and 14 (cooled at 5 °C s^{-1}). In the low-niobium steel there are isolated regions of allotriomorphic ferrite on austenite grain boundaries, which are absent in the microstructure of the higher niobium steel.

The dramatic increase in transformation kinetics resulting from the second-stage austenitization treatments is therefore attributed to the carbide particles which can form during the holding period. The dark-field micrograph and diffraction pattern from such a particle are shown in Fig. 16. They are not at all numerous in the microstructure as a whole. The diffraction pattern may be indexed as a $[\bar{2}\bar{1}1]$ f.c.c. pattern with an approximate lattice parameter of 4.38 Å, close to that of stoichiometric NbC (4.41 Å [17]). Together with the EDX chemical analysis of the particles given

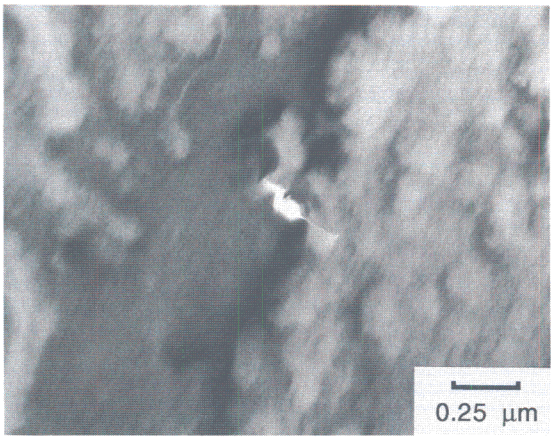

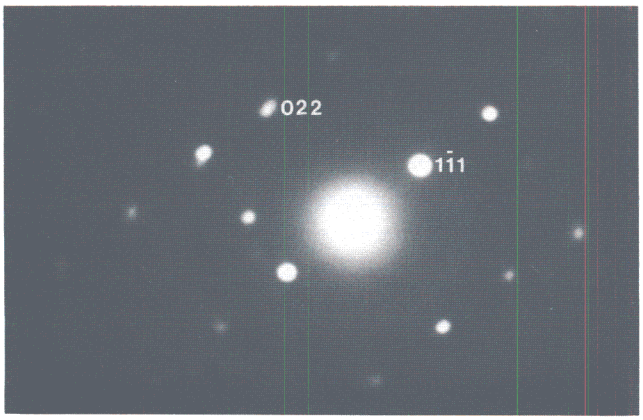

Fig. 16. Dark-field image and diffraction pattern from a niobium carbide or carbo-nitride particle present in steel 4 austenitized as shown in Fig. 2 (held at 950 °C for 460 s), cooled to room temperature at 50 °C s^{-1}.

Table 4
EDX chemical analysis of the particle shown in Fig. 16. Light elements are not detected, and results are normalized to 100%

Element	Nb	Fe	Mn	Si	S
wt.%	98	< 1*	< 1*	< 1*	< 1*

*Measurements not statistically significant relative to background noise.

in Table 4, the particle is therefore identified as a niobium-rich f.c.c. species, probably a carbide or carbo-nitride. These carbides are large compared to the very finely dispersed carbides which precipitate from austenite during rolling of microalloyed steels.

5. Conclusions

The effect of varying the amount of niobium in solid solution on the critical cooling rate to avoid bainite formation appears to be too small to measure using dilatometry. A small effect is observed microstructurally, but this is not sufficient to appear on macroscopic measurements such as dilatation.

It is noticeable, however, that transformation to bainite is retarded by increased niobium in solid solution, but that this effect only becomes apparent at cooling rates slower than V_c. Likewise, by an increase in niobium content, the formation of allotriomorphic ferrite is also suppressed. Niobium's effect when in solid solution therefore seems to be more clearly visible when the driving force for transformation is low.

In comparison, the critical cooling rate is affected significantly by holding the austenite beneath the equilibrium solubility limit for niobium carbide, before cooling. This effect cannot be attributed to changes in the amount of niobium in solid solution but rather to carbide particles forming during the holding period, which in some way enhance bainite formation.

The implications of these results is that, since we have shown that the amount of precipitation necessary to affect transformation is extremely low, it is anticipated that in weld HAZs there will be a large increase in hardenability for regions undergoing thermal cycles for which carbide dissolution is complete, compared to elsewhere in the HAZ. For steels of increasing niobium concentrations, if carbides are fully dissolved, the martensitic hardenability of the resulting austenite should not be greatly affected.

Acknowledgements

The authors are grateful to Sollac (Dunkerque) for funding the project, in particular Mr. F. Sauvage and Mr. G. Sanz. Professor C.J. Humphreys provided the laboratory facilities at the University of Cambridge. Thanks are also due to T. Lemoine and C. Campione at Sollac and Dr. R.C. Thomson at Cambridge.

References

[1] W.B. Morrison, *J.I.S.I., 201* (1963) 317–325.
[2] D. Webster and J.H. Woodhead, *J.I.S.I., 202* (1964) 987–984.
[3] G.L. Fisher and R.H. Geils, *Trans. TMS-AIME, 245* (1969) 2405–2412.
[4] G.T. Eldis and W.C. Hage, *Hardenability Concepts and Application to Steels*, TMS-AIME, Warrendale, PA, 1978, pp. 297–420.
[5] M.H. Thomas and G.M. Michal, in H.I. Aaronson et al. (eds.), *Solid-Solid Phase Transformations*, TMS-AIME, Warrendale, PA, 1981, pp. 469–473.
[6] C. Fossaert, G.I. Rees, T. Maurickx and H.K.D.H. Bhadeshia, *Metall. Trans., 26A* (1993) 21–30.

[7] J.R. Bradley and H.I. Aaronson, *Metall. Trans. A, 12A* (1981) 1729.
[8] H.K.D.H. Bhadeshia and A.R. Waugh, *Solid-Solid Phase Transformations*, TMS-AIME, Warrendale, PA, 1981, pp. 993–998.
[9] H.K.D.H. Bhadeshia and J.W. Christian, *Metall. Trans. A, 21A* (1990) 767–777.
[10] R.R. de Avillez, *Niobium Technical Report*, NbTR, 01/82, CBMM, Brazil, 1982.
[11] French Standard NF A 04-102.
[12] B. Sundmann, B. Jansson and J. Anderson, *Calphad, 9* (1985) 153.
[13] C. Perdrix, B. Chamont, E. Amoris and H. Biausser, *IRSID report, RE 88.322*, IRSID, Paris, July 1988.
[14] E.A. Simielli, S. Yue and J.J. Jonas, *Metall. Trans. A, 23A* (1992) 597–608.
[15] J.J. Jonas and M.G. Akben, *Metals Forum, 4* (1981) 92–101.
[16] S. Yamamoto, C. Ouchi and T. Osuka, in A.J. DeArdo, G.A. Ratz and P.J. Wray (eds.), *Thermomechanical Processing of Microalloyed Austenite*, TMS-AIME, 1982, pp. 613–639.
[17] A.J. DeArdo, J.M. Gray and L. Meyer, in *Proc. Int. Symp. on Niobium, November 1981, San Francisco, CA*, TMS-AIME, 1981, pp. 685–759.